A multi-scale and morphological gradient preserving contrast

Bricola Jean-Charles, Bilodeau Michel and Beucher Serge
MINES ParisTech – PSL Research University
CMM – Centre de Morphologie Mathématique
77300 Fontainebleau, France
jean-charles.bricola@mines-paristech.fr

Introduction

This document outlines an algorithm which extends and enhances the regularised gradient introduced in [Rivest, 1992]. The regularised gradient is known to be a thin gradient. It has little noise, is multi-scale and therefore has been extensively used, for instance in the extraction of road markers [Beucher, 1990] from particularly challenging images. However, the intensity values taken by the regularised gradient are usually not representative of the perceived contrast between objects boundaries. This limitation may be problematic to some applications, because hierarchical segmentations obtained by means of waterfalls or synchronous flooding mechanisms on such a gradient would not match the human perception, since the hierarchy depends on the gradient first overflow zones. The proposed enhancement of the regularised gradient preserves the thinness and multi-scale properties of the latter whilst taking account of the actual contrast across different image scales.

The Algorithm

The computation of the proposed gradient as well as the regularised gradient is performed using the algorithm presented in table 1. Common to both variants, the gradient of a grayscale image $\mathbf{I}$ can be computed between the minimum and maximum scales λ_s and λ_e respectively. Furthermore, the scale λ denotes the size of the structuring element used for the dilation δ, erosion ε and opening γ operators.

When computing the regularised gradient, the thick gradient in step 1.1 captures the intensity variations of image $\mathbf{I}$ under scale λ. The top-hat in step 1.2 eliminates the relief crests having a thickness larger than λ in order to remove thick contours which have merged, whilst the erosion in step 1.3 restores the size of a standard gradient. The following observations, which constituted a starting point for the elaboration of our enhanced regularised gradient, have been made:

- The thick gradient in step 1.1 is by definition highly sensitive to noise. In other words, regions which are supposed to be homogeneous but which are affected by noise will get a significant gradient magnitude. When applying the top-hat in step 1.2, all the crests of interest will therefore loose their dynamic. This justifies the strong levelling, also referred to as a sequential levelling when successively employed with dilations and erosions of increasing sizes [Meyer, 2006], of the input image in step 2.1 of our algorithm prior to the computation of the thick gradient.

- The white top-hat in step 1.2 is meant to remove contours which have fused, which therefore should have reached a thickness of 2λ. When choosing a size of λ, the top-hat tends to remove crests where the curvature is significant as well as junction boundaries, hence the choice of 2λ-1 in step 2.4

- The erosion in step 1.3 happens to destroy the contours especially at high scales. Hence this step is just removed from our algorithm. Instead, we search for the ideal transition points in step 2.2 and apply a binary mask on top of the filtered thick gradient in step 2.5.

| **function** COMPUTEMULTISCALEGRADIENT($\mathbf{I}, \lambda_s, \lambda_e$) :	
1 : $\mathbf{G}$ initialised to the size of $\mathbf{I}$ all pixels set to 0.	
2 : **for all** λ **in** $\{\lambda_s, \lambda_s+1, ..., \lambda_e\}$ **do**:	
3 : $\mathbf{G}_\lambda$:= COMPUTEGRADIENTATSCALE($\mathbf{I}, \lambda$)	
4 : $\mathbf{G}$:= sup $\{ \mathbf{G}, \mathbf{G}_\lambda \}$	
5 : **return G**	
▼ **Regularised gradient** ▼	▼ **Enhanced Regularised Gradient** ▼
function COMPUTEGRADIENTATSCALE($\mathbf{I}, \lambda$) :	**function** COMPUTEGRADIENTATSCALE($\mathbf{I}, \lambda$) :
1.1 : $\mathbf{G}_\lambda := \delta_\lambda(\mathbf{I}) - \varepsilon_\lambda(\mathbf{I})$	2.1 : $\mathbf{I}_F$:= Strong levelling on $\mathbf{I}$ up to scale λ
1.2 : $\mathbf{G}_\lambda := \mathbf{G}_\lambda - \gamma_\lambda(\mathbf{G}_\lambda)$	2.2 : $\mathbf{M}_\lambda$:= Binary mask highlighting intensity transition points in $\mathbf{I}_F$
1.3 : $\mathbf{G}_\lambda := \varepsilon_{\lambda\text{-}1}(\mathbf{G}_\lambda)$	2.3 : $\mathbf{G}_\lambda := \delta_\lambda(\mathbf{I}_F) - \varepsilon_\lambda(\mathbf{I}_F)$
1.4 : **return** $\mathbf{G}_\lambda$	2.4 : $\mathbf{G}_\lambda := \mathbf{G}_\lambda - \gamma_{2\lambda\text{-}1}(\mathbf{G}_\lambda)$
	2.5 : $\mathbf{G}_\lambda := \mathbf{G}_\lambda \times \mathbf{M}_\lambda$
	2.6 : **return** $\mathbf{G}_\lambda$

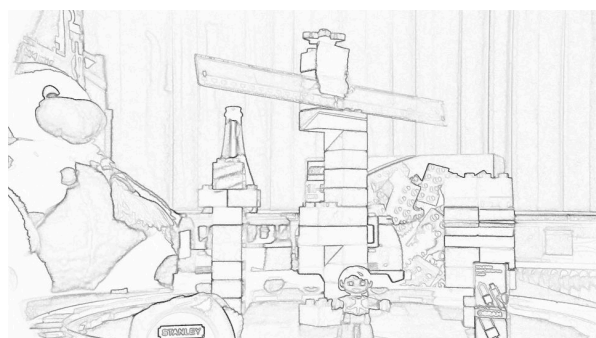Table 1. Algorithm comparison between the regularised gradient and our enhanced gradient

(a) – Input image
Original size: 1920x1080 pixels
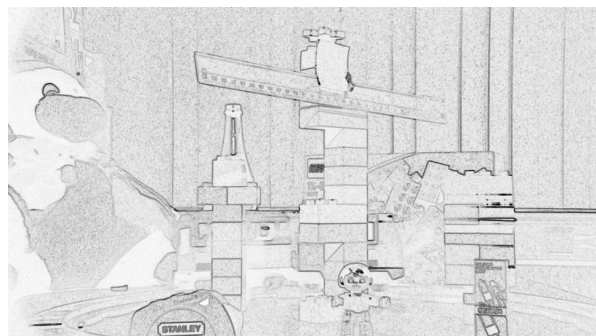
(b) – Morphological gradient (inverted)
of thickness $\lambda=2$
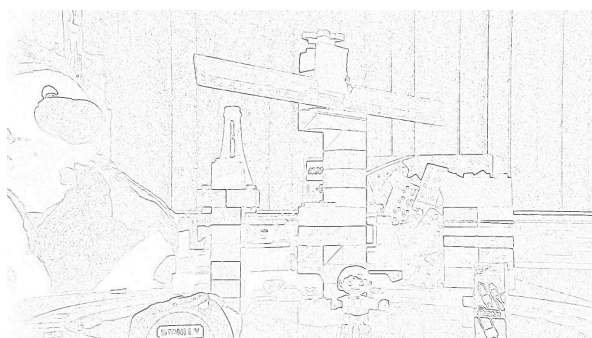
(c) – Regularised gradient (inverted and normalised)
between scales $\lambda_s=2$ and $\lambda_e=10$

(d) – Enhanced regularised gradient (inverted)
between scales $\lambda_s=2$ and $\lambda_e=10$

Figure 1. Comparison of different morphological gradients on colour images

Computing the transition points in step 2.2

Figure 2 illustrates a smooth change of intensity along a scan-line of image **I,** of which the actual intensity step can be captured using a thick gradient of size λ. The transition point corresponds to the intersection of **I** with the morphological average $\frac{1}{2}(\delta_\lambda(\mathbf{I}) + \varepsilon_\lambda(\mathbf{I}))$ when **I** is not flat. In practice however, the equality between the input image and its morphological average is rarely verified.

It is necessary to separate the pixels of the input image **I** into three groups: those above, under or equal to the morphological average. Then, one performs a dilation on **I**, re-classifies the pixels into the three aforementioned groups and searches for those having a different classification. We consider that **I** has been crossed when a pixel changes from an "under" state to an "above" state. We mark this pixel as a transition point as illustrated in figure 3. Symmetrically, we repeat the same process after performing an erosion on **I** and take the union of the detections.
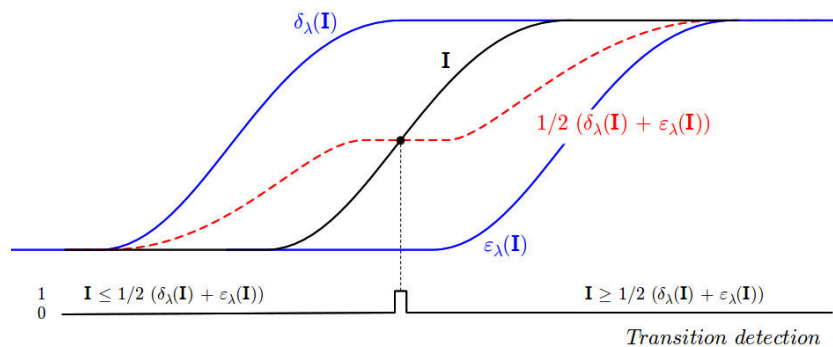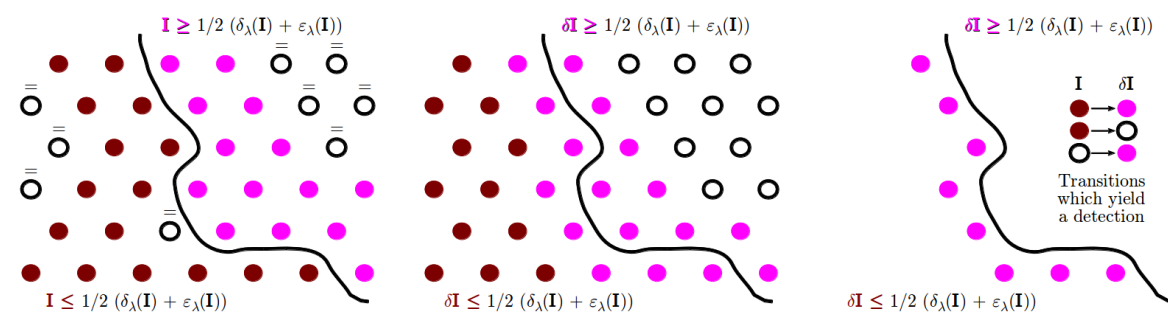
Figure 2. Illustration of the transition point with respect to the morphological average

Red discs denote pixels having a value under the morphological average, purple above and white equal.

Following a dilation on input **I,** red discs denote pixels having a value under the morphological average, purple above and white equal.

State transitions which yield transition points

Figure 3. Illustration of the transition point detection

Jean-Charles Bricola, Michel Bilodeau and Serge Beucher

Results and Discussion

Figure 1 compares three morphological gradients obtained from a colour image which is subject to noise and blurriness. In order to take the colour information into account, we compute the supremum of the gradients for each considered channel. Instead of using the standard red, green and blue channels, we make use of channels which are representative of the perceived brightness [Kalloniatis, 2014] and the image saturation [Demarty, 1998] .

Qualitatively, the enhanced regularised gradient clearly highlights the contours of the train, as well as its wheels, its windows and the railway. One can also better distinguish the legs of the character standing in the middle of the scene. The same goes for the radiator and the electrical plug lying in the background. Finally our gradient is the only one among the three which captures well the strong transition of intensity between the penguin leg and the stomach or the foot.

Finally, the filtering in step 2.1 clearly contributes to the production of a de-noised gradient for $\lambda_s > 1$. It is possible to envisage higher values of λ_s if one is interested in removing contours which are due to textured objects.

Conclusion

We have proposed a revision of the morphological regularised gradient. In its enhanced version, the regularised gradient reflects the perceived contrast between the objects composing a scene. The core of the multi-scale algorithm is identical for both gradients. The principal changes consist of filtering the input image before computing the thick gradient and replacing the erosion by a intensity transition detection for the gradient thinning step. The results attest to the visual appeal of the enhanced gradient which paves the way for the processing and hierarchical segmentation of difficult images.

References

Beucher, S., Bilodeau, M., & Yu, X. (1990, April). Road segmentation by watershed algorithms. In *PROMETHEUS Workshop, Sophia Antipolis, France*.

Demarty, C. H., & Beucher, S. (1998). Color segmentation algorithm using an HLS transformation. *Computational Imaging and Vision*, *12*, 231-238.

Kalloniatis, M., & Luu, C. (2014). Light and dark adaptation. *Webvision: The organization of the retina and visual system*.

Meyer, F. (2006). Levelings: theory and practice. In *Handbook of Mathematical Models in Computer Vision* (pp. 63-78). Springer US.

Rivest, J. F., Soille, P., & Beucher, S. (1992, April). Morphological gradients. In *SPIE/IS&T 1992 Symposium on Electronic Imaging: Science and Technology* (pp. 139-150). International Society for Optics and Photonics.